

On Spread Spectrum for DC grids: Low Frequency Conducted EMI Mitigation and Signal Integrity Disruption in Serial Communication Links

Angel Pena-Quintal, *Student Member, IEEE*, Waseem El Sayed, *Member, IEEE*, Mark Sumner, *Senior Member, IEEE*, Seda Ustun Ercan, *Member, IEEE*, Steve Greedy, *Member, IEEE*, Dave Thomas, *Senior Member, IEEE*, Robert Smolenski, *Member, IEEE*,

Abstract—This paper addresses the effects on nearby communication systems when Spread Spectrum Modulation techniques are used for a DC-DC power converter. These interactions can be found in modern smart grids and automotive power networks in which the combination of communication links, switching power supplies and long cables play a major role in Electromagnetic Interference issues at low frequencies below 150 kHz. Spread Spectrum Modulation, with its different variations (Sine and Random) are widely used to comply with Electromagnetic Compatibility standards. However, there are certain effects that can be harmful to either the converter or the rest of the power network. These effects happen at different frequencies and for different parameters used in the modulation algorithm. With the aim to standardise an assessment procedure, measurements are made to determine the interference created by a SiC based DC-DC converter. The Peak index of a CISPR-16 EMI receiver is used to evaluate the behaviour in the frequency domain while a study in serial communication disruption is undertaken using mean and quantile values from a Bit Error Rate (BER) tester.

Index Terms—dc-dc converter, emi mitigation, low frequency interference, modulation, power quality, spread spectrum.

I. INTRODUCTION

THE recent issues of Electromagnetic Interference at low frequencies created by modern DC-DC power converters are attracting attention due to the lack of Electromagnetic Compatibility (EMC) standardisation at low frequencies and the increasing complexity in electrical and electronic installations. This is because there is an increasing amount of equipment with active switching (often in the form of Switched Mode Power Supplies (SMPS)) resulting in non-negligible emissions in the frequency range between 2 and 150 kHz [1].

Manuscript received Month xx, 2xxx; revised Month xx, xxxx; accepted Month x, xxxx. This work was supported by the European Union's Horizon 2020 MSCA ITN research and innovation programme under the Marie Skłodowska-Curie under Grant 812753 and Grant 812391. (Corresponding author: Angel Pena-Quintal.)

Angel Pena-Quintal, Mark Sumner, Steve Greedy, and Dave Thomas are with the University of Nottingham, Nottingham, UK. (email: angel.penaquintal1@nottingham.ac.uk; mark.sumner@nottingham.ac.uk; steve.greedy@nottingham.ac.uk; dave.thomas@nottingham.ac.uk).

Waseem El Sayed, is with the University of Nottingham, Nottingham, UK and the University of Zielona Gora, Poland. (email: waseem.elsayed@ieee.org).

Seda Ustun Ercan is with the Ondokuz Mayıs University, Samsun, Turkey. (email:sedau@omu.edu.tr)

Robert Smolenski is with the University of Zielona Gora, Poland. (email: r.smolenski@iee.uz.zgora.pl).

There are EMC standards that have been used widely in recent years for AC systems to limit Electromagnetic Interference (EMI) in industrial and scientific applications such as CISPR-11 [2]. For EMI measuring devices, CISPR-16 is the main standard used to address the EMI parameters of electrical and electronic devices for Conducted Emissions between 9 kHz to 30 MHz [3]. The automotive industry is considered in CISPR-25 with frequency limits from 150 kHz to 108 MHz [4]. These standards have in common the allowable limits of emissions in particular applications over different frequency ranges. In order to mitigate the EMI generated by a converter and not exceed these limits, software-based techniques are now being used as an alternative to traditional hardware and filtering techniques as they do not require additional devices or components.

Spread Spectrum Modulation (SSM) has been widely researched as a technique to reduce measured EMI from power converters [5], [6]. SSM is a communication channel optimisation technique that finds its origin in World War II [7]. It decreases the peak energy of a narrowband interfering signal to a broadband interference signal by spreading the waveform energy over a wider frequency range. The graphical explanation of this can be seen in Fig. 1.

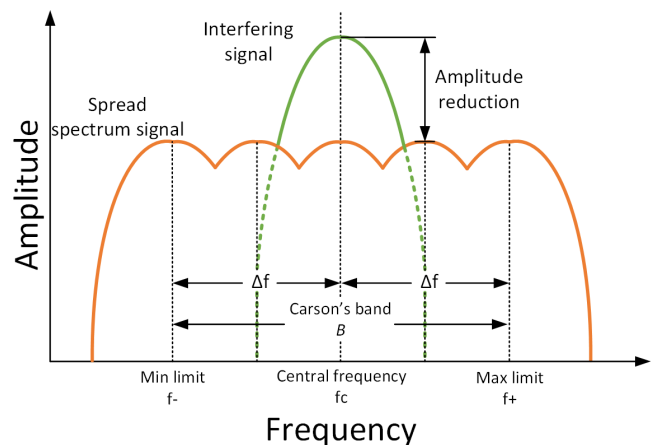


Fig. 1. Spread Spectrum Modulation, the green signal represents the signal to be mitigated, while the orange signal represents the effect of applying Spread Spectrum Modulation.

SSM was initially developed for communications, however the principle can be applied to other fields. In recent research,

it has been suggested that it can be a straightforward way of passing EMC limit tests for devices [8] and can also be applied to reduce power converters emissions. SSM does decrease measured EMI in the frequency-domain up to an acceptable level without additional hardware. This is the main reason why it is accepted by EMC engineers and experts [9]. However, measurements of EMI in the frequency domain alone might not be a full or true measure of the effects of SSM on the electromagnetic emissions of the device [10]. This suggests that other measurement techniques should be considered when evaluating the EMI associated with SSM.

In this paper, the main aim is to generate an understanding of the equipment required to measure emissions in both the time-domain and the frequency-domain for both the source and victim. With this information, a complete assessment can be made of SSM applied to DC converters and its influence on other devices (the EMI victim), the EMI source and the measuring procedure. In addition, this work provides a useful framework to assess the effects of different modulation techniques for DC-DC converters in environments with high noise susceptibility in which cables, converters and frequency switching sources work closely together.

To demonstrate these effects, a combined analysis for SSM with two different driving signals (periodical and non-periodical) is considered. This is to determine the advantages and disadvantages of both approaches in both the time and the frequency domains. Firstly, a complete EMI study of measurements based on the Peak (PK) index is made for the Power Converter using an EMI receiver with frequencies below 150 kHz (CISPR-16 Band A). This analysis will consider the frequency of the driving signal and how this influences the frequency response measured by the EMI receiver. Secondly, the time-domain approach is carried out by analysing Crosstalk generated over a cable bundle placed near the input of the DC converter. The procedure is to measure the errors generated in the cable bundle using the Bit Error Rate (BER) value to analyse the quality of the communication link.

The important contribution of this work is to demonstrate the point at which a considerable degradation (BER increase) of the communication link quality happens when Spread Spectrum is used to decrease the EMI generated in the frequency domain by the power converter (as its source). The focus is on the impact generated by the Crosstalk between nearby lines (power and communication). The results obtained in this work provide important parameters to limit this techniques up to a certain spreading factor, which, can be helpful for future standardisation of the effects of frequency-modulated converters in both time and frequency domains. This is urgently needed for low frequency bands.

To achieve this contribution, this paper is divided as follows. In Section II, the main theory of Spread Spectrum is discussed highlighting the important parameters used to apply this technique in a digital platform. On the measurement side, it also discusses the random generation of frequencies as well as the BER measurement procedure. Finally, this section describes previous work based on Spread Spectrum mitigation techniques focused on wired links. In Section III, the experimental test set-ups are presented considering the two domains

to be analysed. The section includes a complete explanation of the devices involved. The experimental results for the EMI analysis are presented in Section IV, and a comparison of two different modulating signals is discussed. Section V discusses the results obtained from the BER measurements considering the most important parameters to drive the converter using SSM. In addition, this section relates the results and findings of both domains. Finally, Section VI gives the conclusions of this work.

II. SMPS MODULATION AND COUPLED COMMUNICATION LINKS

A. Deterministic Modulation

The usual method to drive a DC-DC converter is with a single fixed frequency, this is often called Deterministic Modulation (DetM). The input voltage and current spectrum of this case will show one peak at the chosen modulation frequency. This peak concentrates most of the energy since it is the main switching harmonic: other peaks will appear at higher switching harmonics as well.

The use of a single frequency can be a drawback for the whole system if proper mitigation techniques such as filtering and shielding are not considered. The baseline switching frequency used in this research work is 50 kHz. This frequency was decided for the reason that it can provide a good alignment with the maximum limit of the CISPR-16 Band A which has a limit at 150 kHz.

B. Spread Spectrum Theory and Main Background

The main idea behind Spread Spectrum is based on common analogue frequency modulation techniques. (1) gives the frequency modulation expression. The fundamental parameters are the modulating frequency ($S(t)$) and carrier signal frequency (w_c).

$$f_{out}(t) = \cos(w_c t + \delta_f \int dt S(t)), \quad (1)$$

δ_f is the frequency deviation from w_c to the frequency of the modulating signal function $S(t)$. The analogue theory of SSM can be used with Carson's band (B) to determine the frequency limits (Fig. 1). This rule refers to a carrier and a modulating signal (2).

$$f_{out} = f_c \pm \frac{B}{2} \cdot \epsilon(t) \quad (2)$$

where B is the frequency range for Carson's band (same as $2 \cdot \delta_f$) based on the spreading range defined for the baseline frequency modulation to be mitigated (f_c). The value of $\epsilon(t)$ is the modulating signal and can be periodical (e.g. sine or triangular) or non-periodical (random and chaotic).

In the case of a non-periodical signal, Pulse Amplitude Modulation (PAM) suggested in [11] and referenced in [12] can be used to generate random patterns as shown in (3). This expression assumes that a digital system with a high clock speed is in charge of the spectrum modulation.

$$\epsilon(t) = \sum_k x_k g(t - kT) \quad (3)$$

where x_k represents the limits given between $[-1, 1]$, the parameter $g(\cdot)$ is the normalized rectangular pulse train between $-1 < t < 0$ and $0 < t < 1$. T is the duration of the pulse. Therefore, by using (3) it is possible to generate a controlled random driving signal on a digital platform. If a periodical signal is used, $\epsilon(t)$ becomes a simple sine or a triangular signal.

Recently, controlled-hybrid algorithms such as those proposed in [13], [14]; and chaotic generation of numbers [15], [16] have been used to mitigate higher levels of EMI when compared to the baseline deterministic case.

However, it should be noticed that there will be trade-offs at higher harmonics that must be considered when implementing this modulation technique. These trade-offs are often neglected by many authors when addressing the impact of Power Quality and Signal Integrity in the time-domain. To develop a practical understanding about the impact of Spread Spectrum for DC/DC converters, the main advantages and disadvantages of this modulation technique as a potential EMI source to communications will be investigated in this paper. This requires the measurement of a given index over a certain time period using different techniques.

Having considered the main background of SSM in [12], the author summarizes SSM as a technique that aims to alter the shape of conducted/radiated emissions interfering with the power spectrum, reducing the level of the peak components as required by international regulations.

C. Modulation index for Frequency Modulation

The parameters that are important when using Spread Spectrum considering (3) or a sinusoidal signal over a digital platform, are the frequency deviation or spreading factor (α), and the sampling frequency of the modulating signal (f_m). The spreading factor is given as the percentage related to the central frequency (f_c) to be modulated.

These two parameters can be considered as a single value which is often referred to as the modulation index (m) for frequency modulation. The comparison of results will be based on the peak closest to the frequency to be mitigated, i.e. the first switching harmonic (for this purpose 50 kHz).

$$m = \frac{\Delta f}{f_m} = \frac{(\alpha \cdot f_c)/2}{f_m} \quad (4)$$

This will provide the same results as for the analogue case given by (5), in which $f_{S(t)}$ is the frequency of the modulating signal.

$$m = \frac{\delta f}{f_{S(t)}} \quad (5)$$

The sampling ratio of the driving signal and the spreading factor can be controlled using a microcontroller with high computational capability or a Field Programmable Gate Array (FPGA). For this research work, the C2000 Texas Instruments microcontroller is used. In order to determine the best possible case to mitigate the effect of the switching frequency for the Device Under Test (DUT), a list of different driving signals and different sampling ratios have been chosen for CISPR-16

Band A for the Resolution Bandwidth (RBW) of the measuring equipment (200 Hz).

If the spreading factor in (4) is fixed at a suitable value and the sampling rate is fixed as well, then Table I shows the different cases to analyse when $\alpha = 45\%$. It is worth mentioning that for the results obtained for lower α , the values of m will be different because the spreading factor decreases.

TABLE I
PLANNED MEASUREMENTS FOR THE EMI RECEIVER WITH $\alpha = 45\%$

EMI Receiver RBW (Hz)	Driving signal	Sampling frequency (Hz)	Modulation index m
200 Hz	Sine or Random	1,000,000	0.01125
		200,000	0.05625
		100,000	0.1125
		20,000	0.5625
		10,000	1.125
		2,000	5.625
		1,000	11.25
		200	56.25
		100	112.5

D. Random Generator: Linear Congruential Generator

The successful mitigation of EMI for a periodical or a non-periodical signal depends mostly on the generation of numbers used as switching frequencies to drive the converter. In digital systems such as FPGAs or microprocessors the effect of pure randomness is difficult to achieve. This is why algorithms to deal with these issues have been developed.

The distribution of random numbers is an important topic. On a normal Gaussian distribution the values close to the mean will repeat more frequently, for linear generators the values generated will have the same probability to appear as the other frequency values in the stream. This can be an advantage over a Gaussian distribution to spread equally the spectrum over the entire bandwidth for frequency domain purposes.

The mathematical expression that controls the generation of the integer random numbers (x_i) is based on the Linear Congruential Generator discovered by Lehmer, according to [17] and is given in (6).

$$x_{i+1} = \text{mod}(Ax_i + B, M) \quad (6)$$

The result of this generator is in the range of $[0, M-1]$ which is usually normalized. The parameters A, B and M affect the period of the stream of numbers. There are other assumptions based on this method to generate random numbers but the algorithm is assumed to provide a linear distribution of switching frequencies for the DC converter. To generate the random pattern that drives the converter, (6) has been programmed in the microprocessor.

E. Fundamentals of measuring BER

To assess the quality of a communication channel in analogue and digital communication links, the BER is used. This parameter will provide a susceptibility figure of merit for a system experiencing external and undesired interference.

The BER measurement is obtained by the division of the Transmitted bits by the Received bits. The generation of the

bit pattern is usually made by Linear Feedback Shift Registers over a certain time or by Amplitude Modulators. The voltage levels can be different from one system to another but the main idea of comparison remains the same.

A BER tester generates a stream of bits for its output and then measures the bits received from the communication channel at its input, this equipment is used to determine the quality of the communication channel. Fundamentally, the comparison of bits is carried out as follows,

$$BER = \frac{N_{err}}{N_{bits}} \quad (7)$$

Considering that the equipment is capable of handling bit counting, one important parameter is the measurement period. This value will provide reliability to the BER measurement. In addition, it helps to have an agreement between measuring devices and protocols. To account for this index, the Confidence Level (CL) value is implemented. This index should consider the period for a measurement and what BER value can be tolerated by the communication system.

By defining this value, a comparison of different modulations can be achieved to finally have a common point for understanding the BER created by frequency modulated DC converters acting as EMI sources. The equation for the Confidence Level is given in (8),

$$CL = 1 - e^{-(N_{bits})x(BER_s)} \quad (8)$$

where, N_{bits} is the total bits transmitted, and BER_s is the maximum allowed BER for the test (usually provided as one standard value). N_{bits} can be calculated as,

$$N_{bits} = \frac{-\ln(1 - CL)}{BER} \quad (9)$$

a the time period needed to achieve a given CL , can be derived as:

$$Time(s) = \frac{-\ln(1 - CL)}{(BER)x(BitRate)} \quad (10)$$

These expressions are used to consider the maximum value of BER allowed on a system for a certain time period. The parameters for the BER experimental tests are given in Table II. A value of 95 % has been used as it is an industry standard rule of thumb [18].

TABLE II
BER CONFIDENCE LEVEL FOR 500 KHZ

Parameter	Value
Ber_{max}	1e-7
Bit Ratio	1e6
CL	95 %

With these parameters, a time period of 30 seconds has been obtained. The frequency of the BER tester has been set at 500 kHz (translated into a value of 1 Mbit/s) as this is the highest value that the equipment can provide, in addition, this frequency is similar to the frequencies used for high speed serial communication and CAN bus links widely used in automotive grids.

F. Spread Spectrum Modulation side effects to communication links

The understanding of Spread Spectrum modulated converters as EMI sources to communication links has been analysed recently thanks to the increasing use and exploitation of smart grids. In the research work of Pareschi [12] et.al., it has been shown that SSM is a mitigation technique used in SMPS that provides a good method to decrease certain interference when compared to DetM. The authors have shown that different driving signals will generate different results and different PK index values when a comparison of periodical and non-periodical driving signals is analysed. These assumptions are true and applicable to the switching harmonics of the DC converter.

For the purposes of this research work, the approach will be similar focusing on the comparison of the first DC Switching Harmonic measured in the bandwidth from 9 kHz to 150 kHz for the DetM, SSM with a Sine signal and SSM with a Random signal.

In [19], there is an analysis of the BER generated by a converter using a two-layer Printed Circuit Board (PCB) in which the traces are close to each other. This represents a similar Crosstalk case to which the experimental tests in this research work are based. In reality, Crosstalk happens when two conductors are close together and one conductor has the potential to interfere with the secondary conductor. Effects like this can be found in smart grids and automotive grids due to the considerable amount of cables without shielding and even in PCB routes. The same authors explored similar options to account for the effect of Spread Spectrum when it is coupled to a standardised communication link. [20], proposed a coupling method based on a capacitor over an I2C communication link. In this work, it has been demonstrated that the BER increases when using different spreading factors for the switching frequency of the DC converter.

What is more, in [21] there is an analysis of the Power Line Communication (PLC) channel performance when a converter with Spread Spectrum is used with a carrier frequency of 63 kHz. In this work, the coupling with a G3-PLC link uses a capacitor. The expected behaviour of decreasing the EMI generated by the converter at the cost of increasing the BER of the communication link was demonstrated.

As was mentioned in the Introduction, the aim of this paper is to create a "rule of thumb" and important recommendations about Spread Spectrum for periodical and non-periodical modulating signals in order to find the best test case or limits with regards to time and frequency domain effects. In [12], the authors suggested that this process can lead to a tuning procedure between the EMI source and the EMI measuring device.

To conclude this section, it is worth mentioning that there will be trade-offs in the SSM usage for DC converters that must be addressed. The advantages of decreasing EMI behaviour are well-know in the frequency-domain, however in the time-domain the application of this modulation can generate issues if the modulation is not developed according to the needs of a device or a whole system.

Having considered the literature review and the recent analysis focused on the frequency-domain for frequency-modulated DC-DC converters it is clear that there is a lack of understanding the drawbacks of these modulation techniques and the main parameters for two different points of view (the source and the victim). In addition there are standardised values provided by the main standards such as PK, Quasi-Peak (QP) and Average (AV) in the frequency domain, but for time-domain analyses, there are not standardised methods to measure the susceptibility effect of SSM for driving converters and nearby systems. Hence, there is a need to analyse time-domain effects and its relation to frequency-domain to minimise the gap in the interpretation of conducted EMI for microgrids, especially for complex systems with complex switching behaviour.

III. EXPERIMENTAL TEST SET-UPS

When working with EMI measurements associated with standards testing, it is important to ensure repeatable measurement conditions. For this work, for each test, the equipment was allowed to reach thermal equilibrium before measurements were made. Also a LISN [22], was used to isolate the measurements from any power system interference for the frequency-domain test.

A. Frequency Domain Set-up

The set-up used in this work has four pieces of equipment. The power supply, the LISN, the EMI Receiver and the Power Converter as the DUT. The block diagram of the set-up is shown in Fig. 2. A brief explanation of the equipment is given as follows.

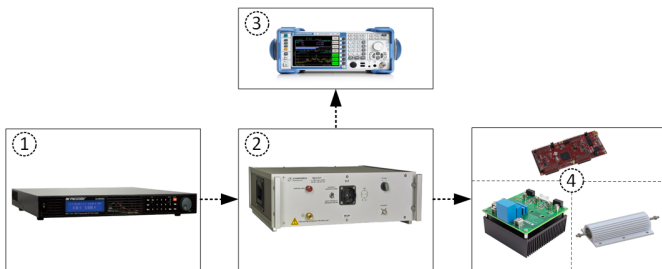


Fig. 2. Experimental setup for the EMI Receiver measurements.

- 1) **Power Supply.** The Power Supply provides 100 V with a maximum current of 14 A.
- 2) **LISN.** The LISN used is the Schwarzbeck NSLK 8127. This LISN is CISPR-16 compliant with a frequency range from 9 kHz to 30 MHz.
- 3) **EMI Receiver.** The EMI Receiver is the R&S ESL3 with a frequency range of 9 kHz to 3 GHz (CISPR-16 compliant).
- 4) **DC Converter.** The DC-DC converter is a half bridge converter with SiC-based Mosfet transistors (manufactured by Wolfspeed). The converter topology is a Synchronous Buck Converter with a base switching frequency of 50 kHz. The converter uses an input capacitor of 5.1 μF and the output capacitor is 470 μF to decrease

the ripple generated and to provide a steady voltage at the output. A Texas Instruments C2000 board is used to generate the SSM patterns, for all of the cases, a 50 % of Duty Cycle is used. The output load of the converter is 10 Ω .

The schematic diagram of the DC-DC converter can be seen in Fig. 3. This block diagram shows how a change can be made for the different domains to be measured with the same DUT.

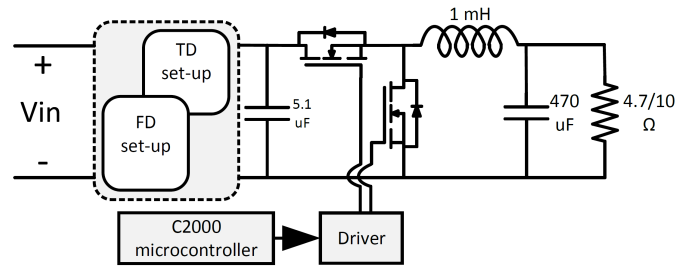


Fig. 3. Circuit schematic of the DC-DC converter used for the experimental tests, this is used for both analyses in time and frequency domain.

The measurement results are based on the PK index value obtained from the EMI Receiver [24]. The parameters of the CISPR-16 Band A are shown in Table III.

TABLE III
CISPR 16 BAND A PARAMETERS

Parameter	Value
Frequency range	9 kHz - 150 kHz
IF Bandwidth	200 Hz
Dwell time	200 ms

B. Time Domain Set-up

For this set-up, the EMI receiver and the LISN are not required. The equipment is based on the power supply, the cable bundle, the Bit Error Rate tester and the DC-DC converter. This set-up is based on a Crosstalk environment in which the cable bundle includes an EMI Source cable and one EMI Victim cable. The block diagram of the set-up is shown in Fig. 4. The same bundle structure has been used in [23] to demonstrate the adverse effect of a Square Fourier Series wave and the BER effect.

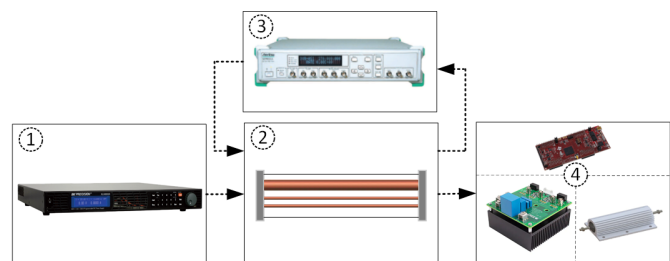


Fig. 4. Experimental setup for the Bit Error Rate measurements.

The brief explanation of the equipment involved is as follows.

- 1) **Power Supply.** The Power Supply is the same as used in the Frequency Domain experimental test set-up.
- 2) **Cable Bundle.** The cable bundle generates a Crosstalk effect between the cables involved. The cable bundle has 3 parallel conductors: two are AWG-36 and they are used for the BER tester data transmission (Data and Data Ground). The other is AWG-14, this is used for the input voltage of the DC-DC converter. By having this cable arrangement, the switching behaviour of the converter modulation will have an interfering effect in the Data Lines, and errors will be generated. The main parameters of the cable bundle can be found in Table IV. The return path of the cable bundle is being generated by means of the ground from the BNC connectors of the BERT.

TABLE IV
CABLE BUNDLE PARAMETERS

Parameter	Value
Distance between cables	1 cm
Height of cables	3 cm
Length of bundle	1.5 m
Connectors (I/O)	BNC

The termination of the cable bundle (input of the BER tester), includes a 50Ω load to match the impedances of the BER tester input by providing signal stability.

- 3) **BER Tester** The BER tester (BERT) is an Anritsu BERT MP8302A. This equipment can generate data with a bit ratio from 1 kHz to 155 MHz. The waveform used is a TTL signal modulated as a Non-Return to Zero (NRZ). For the purposes of this work, the frequency has been set at 500 kHz (10 times the switching frequency).
- 4) **DC Converter.** The DC-DC converter is the same as used previously, with the same components and the same switching frequency parameters. However, the output load has been changed to 4.7Ω to generate more current which is directly translated into a stronger electromagnetic field in the power cable.

IV. EMI: EXPERIMENTAL RESULTS

In this section the results for the experimental tests are discussed. As was pointed out previously (In Table I), there will be two main modulation profiles and nine different sampling ratios, the measured index is the Peak value.

To provide an understanding of how important the driving signal sampling ratios for the SSM scheme are and their relation to the modulation index, two test cases (Sine and Random) of 45 % are shown in Fig 5. This value represents the highest value planned α in the experimental tests. By using a value of 45 %, the spectrum will spread equally in the first half of the frequencies lower than 50 kHz, while the second half of frequencies higher than 50 kHz will have the same effect. A line has been used to highlight the value obtained when DetM was used ($109.74 \text{ dB}\mu\text{V}$).

In Fig. 5, three zones have been highlighted according to the modulation index value, in Zone 1 (light brown), there is a considerable effect of mitigation from the starting point of

the modulation index to $m = 1.125$, in fact the lowest value for both modulating signals can be measured in this point. In Zone 2, a sharply increasing trend is measured from the end of Zone 1 to $m = 11.25$, at this point the Sine wave modulating signal shows almost the same value when compared to DetM while the Random modulating signal is still below the limit given by DetM. Finally, for Zone 3 (dark red), both modulating signals are over the mitigation limit given by DetM. This means that these modulating frequencies must be avoided since no mitigation is achieved. This is mainly caused by the large value of m .

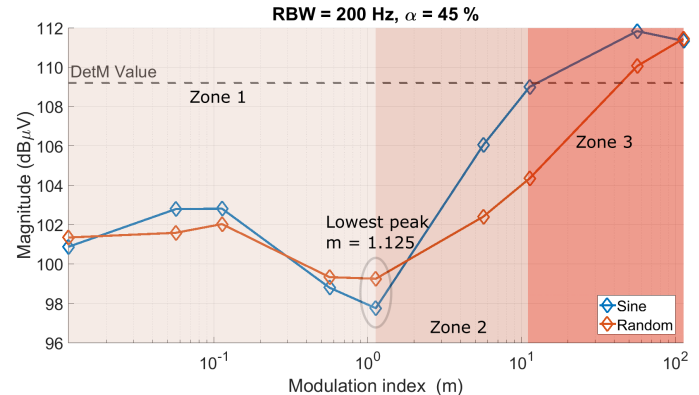


Fig. 5. Measured results of $\alpha = 45 \%$ with the 2 driving signals with different modulation indices.

From the results obtained in Fig. 5, it can be seen that the best values to mitigate the EMI generated by the converter driven by SSM is when m is closest to one or slightly greater.

Having obtained the measurements of the PK index at different values of α and different values for the modulating signal sampling rate (f_m), a cubic interpolation has been used to generate heatmaps in which can be seen the impact of these two important parameters to understand the results from the EMI Receiver. As is suggested in [12], the process to find the best case for optimising the EMI is translated into a tuning process involving both devices, the frequency modulated DC converter and the EMI receiver. This tuning process is made by analysing the results of the interpolation to all of the results measured (5 %, 15 %, 25 %, 35 %, and 45 %).

For simplicity with regards the scaling of the graphs, the heatmaps are shown considering the Sampling Time ($T_s = \frac{1}{f_m}$) of the modulating signal. If the frequency values are needed then the inverse of this value can be calculated.

A. EMI: Sine Wave Signal

The results are gathered together to show the three parameters (Sampling Rate, Spreading Factor and Peak Decrease) on a heatmap that considers 5 %, 15 %, 25 %, 35 % and 45 % for the frequency deviation.

The results obtained for the Sine wave signal are shown in Fig 6. An interesting point to notice is that according to basic knowledge of frequency analysis for modulating signals one might think that the best point to decrease the emissions generated by the switching frequency should be close to 200 Hz because of the RBW of the EMI Receiver. However,

for this case it seems that the best optimisation point is close to 10^{-4} s (10 kHz) which according to the highlighted points is between $203 \mu\text{s}$ and $102 \mu\text{s}$ or in frequency values between 4926 Hz and 9803 Hz.

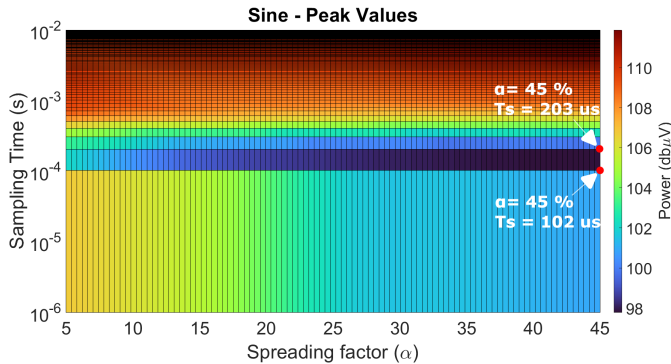


Fig. 6. Heat map for the Sine modulating signal at different Spreading Factors and different Sampling Time.

B. EMI: Random Wave Signal

The results for the Random profile have been obtained in the same way as presented in the last subsection (Sine wave signal). The Random profile measurements can be seen in Fig. 7. In the Random signal graph, the best points to optimise the effect of the interference generated are located between $203 \mu\text{s}$ (4926 Hz) and $102 \mu\text{s}$ (9803 Hz). These are the exact same points as the Sine wave case. This is mainly caused by the use of the same master clock of the microprocessor.

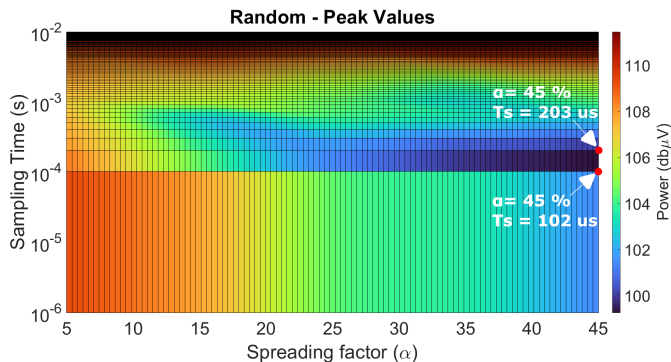


Fig. 7. Heat map for the Random driving signal at different Spreading Factors and different Sampling Time.

Important observations can be discussed in the generation of the heatmaps for different spreading factors. For the extreme case of 45%, a modulation index of 1.145 is obtained with a frequency of 9803 Hz, while for a frequency of 4926 Hz a modulation index of 2.28 is obtained. This can provide an idea about how to tune these parameters in order to find the best value between these limits. This is aligned with the practical values obtained which correspond to the best cases to mitigate EMI, this is by using SSM with a modulation index slightly greater than one. This can be considered as an overmodulation case which is often used to modulate inverters. Interesting observations can be seen when comparing the two

cases, according to the results obtained, the following can be concluded.

- The use of a Sine wave as a modulating signal shows consistent behaviour in the Sampling Time region between 10^{-2} s to 10^{-3} s, while the Random modulating signal starts to decrease the value close to 10^{-4} s with a spreading factor between 15 % and 25 %.
- The Random modulating profile seems to work better over a limited range of spreading factor (from 25 % to 45 %) with a Sampling Time between 10^{-4} s to 10^{-5} s.

To encapsulate all the measurements, the Relative Peak Decrease (RPD) has been calculated using the DetM value as the main point of comparison. These results have been obtained by subtracting the values of the different driving signals with the different parameters. The expression used is given by, $RPD_{peak} = DetM_{peak} - SSM_{peak}$. The results can be seen in Fig. 8. In this figure, the Sine signal shows better performance (approximately $12 \text{ db}\mu\text{V}$) with regards to the Relative Peak Decrease when compared to the Random signal (slightly above $10 \text{ db}\mu\text{V}$). This can lead to the conclusion that Random modulation is worse than usual Periodical modulations, this is considering the assumptions given by the clocking nature of the controlling device (microprocessor).

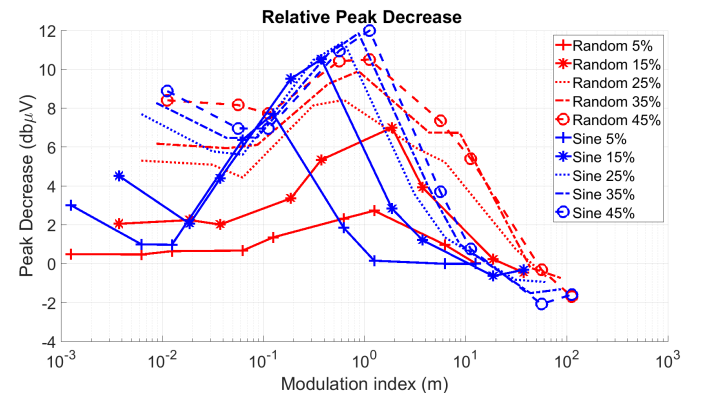


Fig. 8. Relative Peak Decrease for different modulation indices (Higher is better).

V. BER: EXPERIMENTAL RESULTS

The same parameters for FD analysis of Spread Spectrum have been considered for measuring the BER value (time-domain analysis). The number of measurements taken is 100. Every measurement takes 30 seconds (as was suggested in Section II) in order to provide enough time to avoid discrepancies between different cases and to provide stability between values.

A. BER with a Sine/Random Wave Modulating Signal

The results obtained from the BER measurements were analysed statistically. Boxplots were used to demonstrate the non-linear effect of the Spread Spectrum Modulation over the communication link. Similar results were obtained for the different spreading factors. For simplicity in the paper only

TABLE V
ANALYSIS OF BER FOR SPREADING FACTOR OF 45% AND EMI RECEIVER RESULT

m	Sine Wave					Random Wave				
	BER Mean	Q1	Q2	Q3	PK (dB μ V)	BER Mean	Q1	Q2	Q3	PK (dB μ V)
0.01125	1.041E-02	1.040E-02	1.040E-02	1.050E-02	100.86	1.706E-02	1.700E-02	1.710E-02	1.710E-02	101.34
0.05625	1.146E-02	1.140E-02	1.150E-02	1.150E-02	102.78	1.750E-02	1.750E-02	1.750E-02	1.750E-02	101.58
0.1125	1.289E-02	1.290E-02	1.290E-02	1.300E-02	102.80	1.773E-02	1.770E-02	1.770E-02	1.780E-02	102.02
0.5625	1.193E-02	1.190E-02	1.190E-02	1.200E-02	98.79	1.312E-02	1.310E-02	1.310E-02	1.320E-02	99.32
1.125	1.203E-02	1.195E-02	1.210E-02	1.230E-02	99.10	9.491E-03	9.470E-03	9.490E-03	9.510E-03	99.24
5.625	1.305E-02	1.300E-02	1.300E-02	1.310E-02	106.04	8.493E-03	8.440E-03	8.485E-03	8.550E-03	102.4
11.25	1.311E-02	1.310E-02	1.310E-02	1.310E-02	108.99	8.550E-03	8.460E-03	8.550E-03	8.635E-03	104.34
56.25	1.320E-02	1.320E-02	1.320E-02	1.320E-02	111.82	8.624E-03	8.460E-03	8.620E-03	8.765E-03	110.05
112.5	1.315E-02	1.310E-02	1.310E-02	1.320E-02	111.33	9.471E-03	9.240E-03	9.490E-03	9.695E-03	111.44

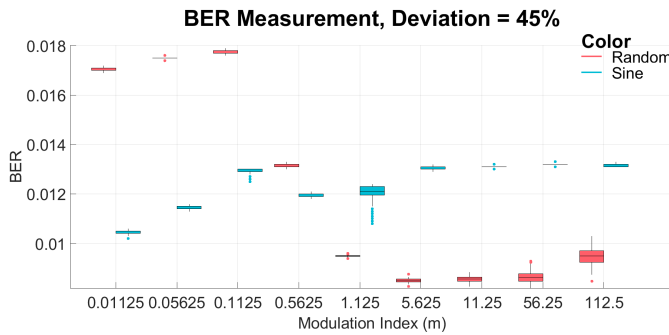


Fig. 9. Boxplot comparing Sine and Random waves with different modulation indices.

the highest case of 45 % is shown in Fig. 9 with the Boxplot charts.

As can be seen in Fig. 9, the use of Random modulation presents an interesting change of its trend when the modulation index is close to zero. The BER measured at $m = 0.01125$ was approximately 0.017 while at $m = 0.5625$ the error was 0.01. This represents a change of BER of almost 90 %. Another important observation that is seen is the trend in the results for the sine wave when the value of m changes from values below one to values greater than one.

In Table V, a summary of the analysed results is given for the two different modulating signals (with $\alpha = 45\%$) as well for the different spreading factors and for the modulating frequencies of the driving signals. In this table, the mean values and the quantile values (Q1, Q2 and Q3) are obtained for the BER while the last column includes the PK index value.

The lowest values for the PK index are highlighted in bold text. An interesting point to mention is the effect on the BER which changes its value considerably when the modulating index is greater than one.

In fact, for a Sine wave modulating signal at $m = 0.5625$ a value of 98.79 dB μ V has a BER of 1.193E-2. What is interesting is that there is a change of trend that settles after this point. For a Random wave modulating signal, at $m = 1.125$, a value of 99.24 dB μ V has a BER of 9.491E-3, this shows a change of trend from higher to lower values in the measured BER.

B. Results: BER vs Spreading Factor (α)

To provide a useful understanding about the effects of the two modulating signals used for the SSM, the average values of all of the measurements have been calculated. The graph showing the modulating index and its relation to the BER is shown in Fig. 10.

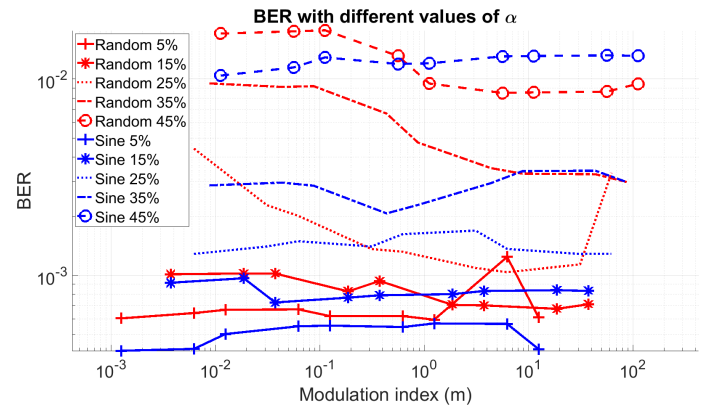


Fig. 10. Average values of BER for the different spreading factors with different modulation indices.

In Fig. 10, the expected results of increasing the spreading factor will increase the BER measured. However, there are interesting cases in which Random and Sine driving signals will perform similarly. This applies slightly differently for the five cases presented but it does happen, especially for spreading factors greater or equal than 25 %.

C. BER vs Peak Decrease

Finally, in an effort to find the relation between the BER and the Peak Decrease and to determine the point at which the considerable drawback effect happens, two graphs with all the results are plotted considering the relative values of both measurements. The relative values consider the results obtained by means of DetM and subtracting these to the Spread Spectrum modulated cases. The results can be seen in Fig. 11 for the Sine wave modulating signal, while Fig. 12 shows the results for the Random wave modulating signal. The maximum limit for every α obtained has been highlighted in red.

In these graphs, it can be seen that the Sine modulating signal shows a steady performance and stability with regards

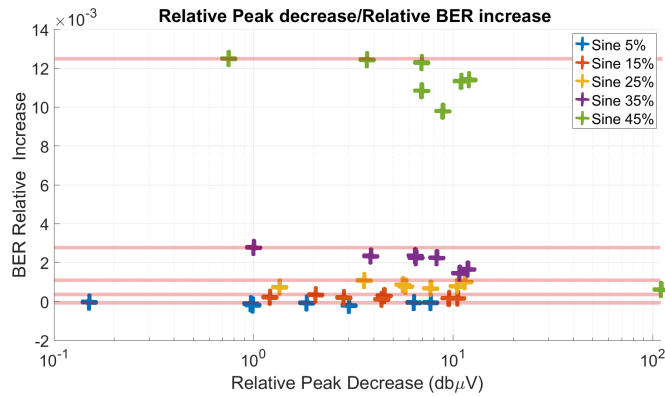


Fig. 11. Sine wave, relative Peak decrease and relative BER increase.

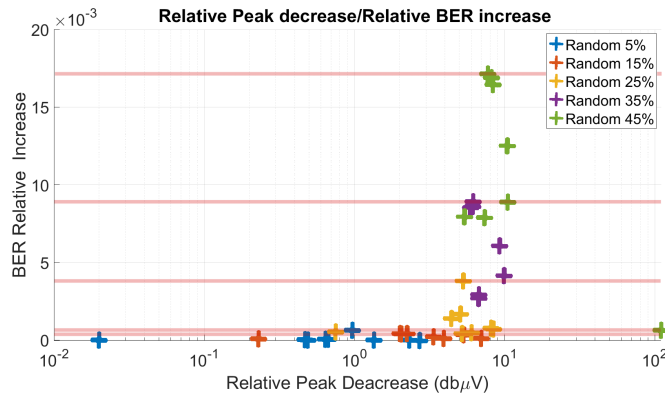


Fig. 12. Random wave, relative Peak decrease and relative BER increase.

to BER and EMI Peak decrease from 5 % to 35 %. What is interesting is the big change when the spreading factor is changed to 45 %, as both indices increase considerably.

On the other hand, when the Random modulating signal is used, an interesting trend develops with the increasing values of the spreading factor and its impact on the Relative Peak Decrease. There is a continuous increase of the relative BER. From 5 % to 25 % the effect of mitigation is steady, while this trend changes sharply from 35 % to 45 %.

In summary, the effect of increasing the spreading factor and consequently increasing the modulation index will generate a considerable BER degradation point for both signals when $\alpha > 25\%$ as highlighted in red in both graphs (Fig. 11 and Fig. 12). This value can be used as a limit or a reference for not surpassing when considering the benefits of Spread Spectrum as a mitigation technique.

VI. CONCLUSION

This paper has demonstrated the well-known advantages of SSM as a mitigation technique for DC-DC power converters in the frequency domain. The expected behaviour of EMI decrease applies, i.e. the higher the spreading factor the lower the peak measured. This is true when compared to the same converter using DetM. However, the effect of an increase in the spreading factor increases the BER value (of the coupled environment) if we compare SSM with DetM.

Another important point to mention is, when Sine and Random driving signals are compared (without considering DetM), interesting trends can be found when the modulation index factor is greater than one. For a Sine wave, there is a small dip that settles after the increasing trend in this value, while for a Random wave there is a big change when the modulation index is closer to values greater than one. In fact, it seems that a bit of overmodulation can provide good results to decrease the EMI whilst not affecting the BER substantially depending on the spreading factor used.

The measured results have shown that there exists one point (values close to one) in which the frequency domain best mitigation point can be obtained by not affecting considerably the BER value when periodical and non-periodical driving signals are compared. This can be helpful for design engineers to account for the modulation cases that do not impact the quality of the communication without reducing the positive effects of SSM in the frequency domain for the CISPR Band A under test.

The approach presented in this paper can be considered to be a framework of measurements for future standardisation to address two different domains with the same DUT.

REFERENCES

- [1] Sarah K. Rönnerberg et al., "On waveform distortion in the frequency range of 2kHz – 150kHz — Review and research challenges", *Electric Power Systems Research*, Volume 150, 2017, Pages 1-10.
- [2] CISPR-11-6, Industrial, scientific and medical equipment - Radio frequency disturbance characteristics - Limits and methods of measurement - Requirements for air-gap wireless power transfer (WPT). International Electrotechnical Commission, 2016.
- [3] CISPR-16-3, Specification for radio disturbance and immunity measuring apparatus and methods Part 1-1: Radio disturbance and immunity measuring apparatus – Measuring apparatus. International Electrotechnical Commission, 2010.
- [4] CISPR-25, Radio disturbance characteristics for the protection of receivers used on board vehicles, boats, and on devices - Limits and methods of measurement, 2nd ed, 2002
- [5] J. Balcells, A. Santolaria, A. Orlandi, D. Gonzalez and J. Gago, "EMI reduction in switched power converters using frequency Modulation techniques," in *IEEE Transactions on Electromagnetic Compatibility*, vol. 47, no. 3, pp. 569-576, Aug. 2005, doi: 10.1109/TEMC.2005.851733.
- [6] F. Pareschi, G. Setti, R. Rovatti and G. Frattini, "Practical Optimization of EMI Reduction in Spread Spectrum Clock Generators With Application to Switching DC/DC Converters," in *IEEE Transactions on Power Electronics*, vol. 29, no. 9, pp. 4646-4657, Sept. 2014, doi: 10.1109/TPEL.2013.2286258.
- [7] R. Scholtz, "The Origins of Spread-Spectrum Communications," in *IEEE Transactions on Communications*, vol. 30, no. 5, pp. 822-854, May 1982, doi: 10.1109/TCOM.1982.1095547.
- [8] M. Stecher, "Possible effects of spread-spectrum-clock interference on wideband radiocommunication services," 2005 International Symposium on Electromagnetic Compatibility, 2005. EMC 2005., 2005, pp. 60-63, doi: 10.1109/IEMC.2005.1513472.
- [9] H. G. Skinner and K. P. Slattery, "Why spread spectrum clocking of computing devices is not cheating," 2001 IEEE EMC International Symposium. Symposium Record. International Symposium on Electromagnetic Compatibility (Cat. No.01CH37161), 2001, pp. 537-540 vol.1, doi: 10.1109/IEMC.2001.950699.
- [10] R. Mukherjee, A. Patra and S. Banerjee, "Impact of a Frequency Modulated Pulsewidth Modulation (PWM) Switching Converter on the Input Power System Quality," in *IEEE Transactions on Power Electronics*, vol. 25, no. 6, pp. 1450-1459, June 2010, doi: 10.1109/TPEL.2009.2037421.
- [11] S. Callegari, R. Rovatti and G. Setti, "Spectral properties of chaos-based FM signals: theory and simulation results," in *IEEE Transactions on Circuits and Systems I: Fundamental Theory and Applications*, vol. 50, no. 1, pp. 3-15, Jan. 2003, doi: 10.1109/TCSI.2002.807510.

- [12] F. Pareschi, R. Rovatti and G. Setti, "EMI Reduction via Spread Spectrum in DC/DC Converters: State of the Art, Optimization, and Trade-offs," in *IEEE Access*, vol. 3, pp. 2857-2874, 2015, doi: 10.1109/ACCESS.2015.2512383.
- [13] O. Trescases, G. Wei, A. Prodic and W. T. Ng, "An EMI Reduction Technique for Digitally Controlled SMPS," in *IEEE Transactions on Power Electronics*, vol. 22, no. 4, pp. 1560-1565, July 2007, doi: 10.1109/TPEL.2007.901911.
- [14] A. Pena-Quintal, K. Niewiadomski, S. Greedy, M. Sumner and D. Thomas, "The Influence of the Number of Frequencies and the Frequency Repetitions Rates in Spread Spectrum Sigma-Delta Modulated DC-DC Converters," 2021 Asia-Pacific International Symposium on Electromagnetic Compatibility (APEMC), 2021, pp. 1-4, doi: 10.1109/APEMC49932.2021.9597184.
- [15] F. Pareschi, G. Setti, R. Rovatti and G. Frattini, "Short-term Optimized Spread Spectrum Clock Generator for EMI Reduction in Switching DC/DC Converters," in *IEEE Transactions on Circuits and Systems I: Regular Papers*, vol. 61, no. 10, pp. 3044-3053, Oct. 2014, doi: 10.1109/TCSI.2014.2327273.
- [16] G. Marsala and A. Ragusa, "Chaos PWM for EMI reduction in a high boost DC-DC converter with coupled inductors," 2017 IEEE 5th International Symposium on Electromagnetic Compatibility (EMC-Beijing), 2017, pp. 1-6, doi: 10.1109/EMC-B.2017.8260349.
- [17] R. S. Katti and R. G. Kavasseri, "Secure pseudo-random bit sequence generation using coupled linear congruential generators," 2008 IEEE International Symposium on Circuits and Systems, 2008, pp. 2929-2932, doi: 10.1109/ISCAS.2008.4542071.
- [18] Keysight, "How to Measure Bit Error Rate (BER)" [online]. Available at: <https://www.keysight.com/zz/en/assets/7018-06435/white-papers/5992-3524.pdf>
- [19] F. Musolino and P. Crovetto, Interference of Spread-Spectrum Switching-Mode Power Converters and Low-Frequency Digital Lines, IEEE International Symposium on Circuits and Systems (ISCAS), 2018.
- [20] P. Crovetto and F. Musolino, Interference of Spread-Spectrum EMI and Digital Data Links under Narrowband Resonant Coupling, *MDPI Electronics* 2020, 9, 60.
- [21] W. E. Sayed, P. Lezynski, R. Smolenski, N. Moonen, P. Crovetto, and D. W. P. Thomas, "The Effect of EMI Generated from Spread-Spectrum-Modulated SiC-Based Buck Converter on the G3-PLC Channel," *Electronics*, vol. 10, no. 12, p. 1416, Jun. 2021, doi: 10.3390/electronics10121416.
- [22] F. A. Kharanaq, A. Emadi and B. Bilgin, "Modeling of Conducted Emissions for EMI Analysis of Power Converters: State-of-the-Art Review," in *IEEE Access*, vol. 8, pp. 189313-189325, 2020, doi: 10.1109/ACCESS.2020.3031693.
- [23] M. J. Basford, C. Smartt, D. W. P. Thomas and S. Greedy, "On the disruption of wired serial communication links by time domain interference," 2018 IEEE International Symposium on Electromagnetic Compatibility and 2018 IEEE Asia-Pacific Symposium on Electromagnetic Compatibility (EMC/APEMC), 2018, pp. 183-186, doi: 10.1109/ISEMC.2018.8393763.
- [24] D. Schwarzbeck, "The EMI-Receiver according to CISPR 16-1-1", Schwarzbeck Mess-Elektronik.



Angel Pena-Quintal was born in Yucatan, Mexico. He received his master's degree in Electronics, Signal Processing and Communications from the University of Seville, Spain in 2017, and the bachelor's degree in Mechatronics Engineering from the University of Yucatan in 2014. Since October 2019, he is working towards the PhD degree at the University of Nottingham at department of the Electrical and Electronic Engineering. His research interests are focused on Electromagnetic Interference for power converters and grids in renewable energy sources and the analysis of Power Quality and Signal Integrity in microgrids.



Netherlands and University of Nottingham, United Kingdom.

Waseem El Sayed was born in 1991, in Alexandria, Egypt. He finished his B.Sc. and M.Sc. studies in electrical and control engineering from the Arab Academy for Science and Technology and Maritime Transport (AASTMT), Egypt in 2013, and 2018 respectively. In April 2019, he started his Ph.D. studies as an Earlier Stage Researcher number 1 in the "SCENT - Smart Cities EMC Network for Training" project, he was recruited for the joint degree Ph.D. between three unique universities: University of Zielona Gora, Poland, University of Twente,



systems, including sensorless motor drives, diagnostics and prognostics for drive systems, power electronics for enhanced power quality, and novel power system fault location strategies.

Mark Sumner (Senior Member, IEEE) received the B.Eng. degree in electrical and electronic engineering from the University of Leeds in 1986, and the Ph.D. degree in induction motor drives from the University of Nottingham, U.K., in 1990. He was with Rolls Royce Ltd., U.K. He was also a Research Assistant and a Lecturer in October 1992. He is currently a Professor of Electrical Energy Systems with the Power Electronics, Machines and Control Group, University of Nottingham. His research interests include control of power electronic



Seda Ustun Ercan was born in Turkey. She received the B.S, M.Sc. and Ph.D. degrees in electrical and electronic engineering from Ondokuz Mayıs University, Samsun, Turkey, in 2005, 2009 and 2016, respectively. She was a Postdoctoral researcher in electrical and electronic engineering from the University of Nottingham in United Kingdom. She is currently an Assistant Professor at the department of electrical and electronics engineering in Samsun, Turkey. Her research interests include power line communication and digital signal processing.



Steve Greedy (Member, IEEE) received the MEng and PhD degrees in 1998 and 2002 from the University of Nottingham. He is Assistant Professor within the George Green Institute for Electromagnetics research. His research interests are in the area of experimental and computational electromagnetics with a focus on techniques used in the study of electromagnetic compatibility and signal integrity, specifically mechanisms that impact performance of wired and wireless communication systems.



Dave Thomas (Senior Member, IEEE) received the B.Sc. degree in physics from Imperial College, London, U.K., in 1981, the M.Phil. degree in space physics from Sheffield University, Sheffield, U.K., in 1984, and the Ph.D. degree in electrical engineering from Nottingham University, Nottingham, U.K., in 1990. He is a Professor of electromagnetics applications with the George Green Institute for Electromagnetics Research, The University of Nottingham, Nottingham, UK. He is a member of CIGRE and Convenor for Joint Working Group C4.31 EMC

between communication circuits and power systems, Chair of COST Action IC 1407 "Advanced characterisation and classification of radiated emissions in densely integrated technologies," a member of several conference committees, and the EMC Europe International Steering Committee. His research interests include electromagnetic compatibility, electromagnetic simulation, power system transients, and power system protection.



Robert Smolenski (Member, IEEE) was born in 1973 in Krosno Odrzanskie, Poland. He received the M.Sc., Ph.D., and Postdoctoral degrees in electrical engineering from the University of Zielona Gora, Zielona Gora, Poland. He is currently an Associate Professor and the Head of the Institute of Automatics, Electronics and Electrical Engineering, University of Zielona Gora, and the Deputy Chair of the Joint IEEE IES/PELS Poland Chapter as well as a Member of the Electromobility Board of the National Centre for Research and Development. His

research focuses on issues linked with the assurance of power quality as well as the interoperability of power systems involving power electronic interfaces and control arrangements.